energies

MDPI

Article

Dynamic Simulation of a Gas and Oil Separation Plant with Focus on the Water Output Quality

Thorsten Jonach *, Bahram Haddadi, Christian Jordan and Michael Harasek

TU Wien, Institute of Chemical, Environmental and Bioscience Engineering, Getreidemarkt 9/166, 1060 Wien, Austria

* Correspondence: thorsten.jonach@tuwien.ac.at

Abstract: Gas and oil separation plants are the first main step in the production of hydrocarbon products. Depending on the properties of the recovered components from the well heads, and the physical properties in the underground rock reservoir, the plant design can vary in different ways. In mature oil and gas fields, secondary recovery methods are often used, which include the injection of large amounts of water into the underground reservoir, to induce the production flow of the wells. The handling of this water is of significant interest, in terms of production efficiency and pollution reduction, because the water comes into contact with the environment during and after recovery operations. In this work, a model of an exemplary gas and oil separation plant was created in Aspen HYSYS V10. A particular focus was placed on the modeling of oil residues in the water-bearing plant components. This model was then extended by the implementation of different process control schemes, to create a predictive model that could represent dynamic operating states in the plant components. Two different dynamic changes were then simulated using this model, to showcase the capabilities and capacities of the model.

Keywords: process simulation; plant dynamics; process integration; oil production

Citation: Jonach, T.; Haddadi, B.; Jordan, C.; Harasek, M. Dynamic Simulation of a Gas and Oil Separation Plant with Focus on the Water Output Quality. *Energies* **2023**, *16*, 4111. https://doi.org/10.3390/en16104111

Academic Editors: Antonio Zuorro, Athanasios I. Papadopoulos and Panos Seferlis

Received: 16 March 2023
Revised: 9 May 2023
Accepted: 11 May 2023
Published: 16 May 2023

1. Introduction

The fluid which is recovered at the well heads in oil and gas fields consists of several components that are in different states of aggregation. The quantities of the different phases, as well as the solids that exist in the recovered mixtures depend on the production method, and on the physical properties of the oil reservoir and the composition of the recovered fluid. The first processing step for the extracted mixture is usually the gas and oil separation plant. The main purpose of this plant is to separate the majority of the components. The involved streams undergo different separation steps, until the desired separation quality is achieved. The segregated oil and gas streams are then fed to subsequent processing plants for further production, whereas the segregated water stream undergoes different cleaning processes.

The separation process in gas and oil separation plants is carried out in subsequent separation stages. Simulation-driven optimization of such plants plays an important role in the optimization and analysis of processes in oil and gas production. The selection of optimal pressure for the multi-stage separation units in gas and oil separations is an important task in order to optimize recovery and enhance production efficiency. Olsen et al. [1] used a process simulation model and a CMA-ES (covariance matrix adaptation evolution strategy) algorithm to study the optimal parameters in multi-stage separation for different incoming fluids. Mahmoud et al. [2] used a dynamic simulation model and neural networks to determine the optimal pressure for each stage separation in terms of extra oil recovery. The dynamic changes in pressure, level heights, and outflow in certain units in the process have been investigated in previous works [3]. For the optimization of certain plant infrastructures, the analytical RTO strategy offers numerous advantages

over conventional methods. This strategy permits real-time optimization of the process, leading to substantial enhancements in process performance, energy efficiency, and product quality, and could therefore contribute to optimization, in combination with a rigorous model of a gas and oil separation plant [4]. The different separation equipment, such as three-phase separators, involved in such a process has been studied in various works [5]. The dynamic behavior of three-phase separators, which are heavily utilized in gas and oil separation plants, has been previously studied by solving a set of differential and algebraic equations [6]. To take into account the liquid–liquid separation efficiencies under dynamic conditions in such devices, modeling approaches have been used that utilize the gravity settling of dispersed particles from a continuous phase [7]. More sophisticated models for liquid–liquid gravity separation also take into account the evolution of the dispersed phase during separation by utilization of a population balance model [8]. The combination of these techniques has been studied on three-phase separation equipment, to estimate separation efficiencies and dynamic parameters, such as pressure and level height [9,10]. Effects on droplet evolution under various conditions, using computational fluid dynamics, provide better information about the overall behavior of the dispersions in the process [11]. Computational fluid dynamics is heavily utilized, to study and optimize the phase interactions during gravity separation [12,13]. The implementation of population balance models in computational fluid dynamic codes provides an even better insight into the separation process [14]. The disadvantage of CFD is primarily the high computational effort, which is not suitable for some application areas, such as large-scale project planning or monitoring of an overall plant.

As recovery operations in underground oil reservoirs often depend on the initiation of certain physical parameters in the rock formation to induce a flow and pressure gradient, secondary recovery methods, like water injection, are often used. To induce a flow at the well heads, water is injected into the rock formation at an injection point, and the reservoir mixture is then recovered at the production wells. This method also introduces a large amount of water, especially in mature oil fields, to the production circle, which needs to be handled in the downstream separation processes [15]. The produced water is then used for re-injection and further recovery, or can be stored in already exploited regions in the rock formation: in both cases, the high purity of the water must be guaranteed. When the produced water is re-injected into the reservoir, eventual impurities can alter the water's viscosity, and lead to the reduction of recovery efficiency [16]. Contaminated water can also impact the environment when stored in underground rock formations; therefore, at all stages of production, great importance must be attached to the efficiency of the separation, with a focus on water quality. Furthermore, due to the large amount of water used for the exploitation of mature oil and gas fields, the separation units are highly susceptible to dynamic changes. These dynamic changes must be considered, in order to adequately adjust the operating parameters of the plant, and the design of the separation units, so as to reduce oil impurities in the produced water.

Although there are numerous modeling approaches available in the literature for gas and oil separation plants, there is a lack of specific models dedicated to the determination of oil residues in the produced water. The motivation for this work was to create an approach for process simulation of oil and gas separation plants, in order to give a more detailed insight into the modeling of dynamic processes and plants in the process simulation software Aspen HYSYS. The focus of this modeling approach is the prediction of possible residual oil contaminations and their dynamic changes in the produced water system of such plants. The modeling strategies presented could be used to create predictive models of real-life gas and oil separation plants in the industry.

2. Methods and Materials

The first step in the gas and oil separation plant model is the three-phase separation of the incoming water, oil, and gas streams. In addition, a large part of the solids that are entrained in the stream, due to the flushing of the reservoir, is separated in this step. The separation units usually consist of a horizontal vessel with specific inlet devices that separate the bulk amount of the vaporous phase at the inlet. The remaining liquid mixture is then transferred to the gravity separation part of the vessel, where the different components are separated according to their respective densities. The lighter liquid is then transferred over the weir to the second section, where it is recovered for further production. Additionally, such units are equipped with specific devices in the liquid–liquid separation area, to boost the liquid–liquid separation efficiency and to introduce foam-breaking in the liquid phase. Due to the large amount of water in the process, the height of the water and oil level setpoints in the gravity settling area must be accorded great importance. Under dynamic conditions, fluctuations in the water level occur in such systems, which can lead to an overflow of water in the oil recovery section, or to poor separation of oil residuals in the water; therefore, gas and oil separation plants usually consist of multi-stage separation operations under various operating pressures. The number of separation units can vary in this process, and dynamic deviations in the individual separation steps can thus be unevenly distributed over the entire process. An exemplary gas and oil separation plant layout can be seen in Figure 1.

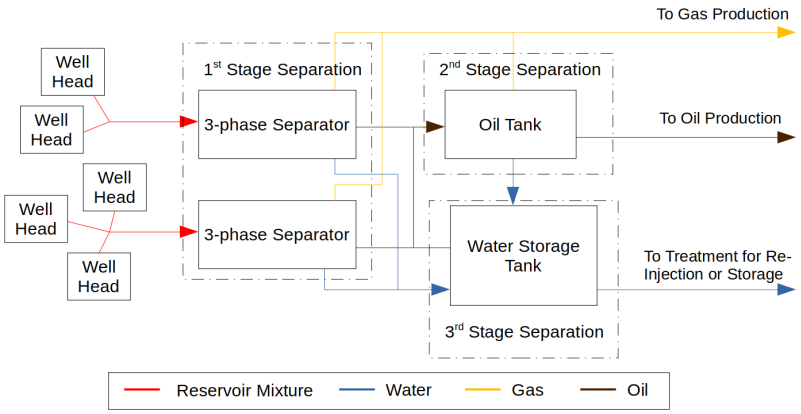

Figure 1. Layout of a gas and oil separation plant with three-stage separation.

As shown in Figure 1, the reservoir fluid undergoes different separation stages. At all stages, the involved process water has contact with impurities, such as oil residuals, which are meant to be separated. The dynamic behavior of the different parameters, and the dynamics in the control and layout of the different separators, impact the overall quality of the discarded water. This work aims to analyze the dynamic behavior and to simulate the evolution of oil residuals in the water output phase during the operation.

3. Flowsheet Model

For the creation of the model, Aspen HYSYS V10 [17] was used. The plant layout was chosen as in Figure 1, with two parallel three-phase separators in the first separation stage. The water outlet of the separators was then directly transferred to the third-stage separator, whereas the oil outlet was transferred to the second separation stage. The oil output of this second separation stage was then transferred for further processing, and the water residuals were turned over to the third separation stage. As initial conditions, the composition of the fluids fed from the well head into the first separation stage was assumed to be 0.91 for water, 0.047 for oil, and 0.043 for gas.

The overall flowsheet can be seen in Figure 2. The three main separation stages are referred to as vessel V-100 (referred to as Separator 1) and V-103 (referred to as Separator 2) for the first-stage three-phase separators, V-101 for the second-stage separation, and V-102

for the final-stage separation. It is important to note that in order to fully validate and adapt the modeling approach to a real-life plant, actual data from the plant is required. In addition, the use of different data reconciliation strategies can enable various applications in the field of predictive modeling, such as virtual sensing techniques [18] or process evaluation studies [19]. Therefore, obtaining data for validation and data reconciliation purposes should be considered a crucial step in the adaptation of the modeling approach in order to generate a more reliable predictive model. The following section specifies the used properties for the respective separation stages for demonstration of the modeling approach.

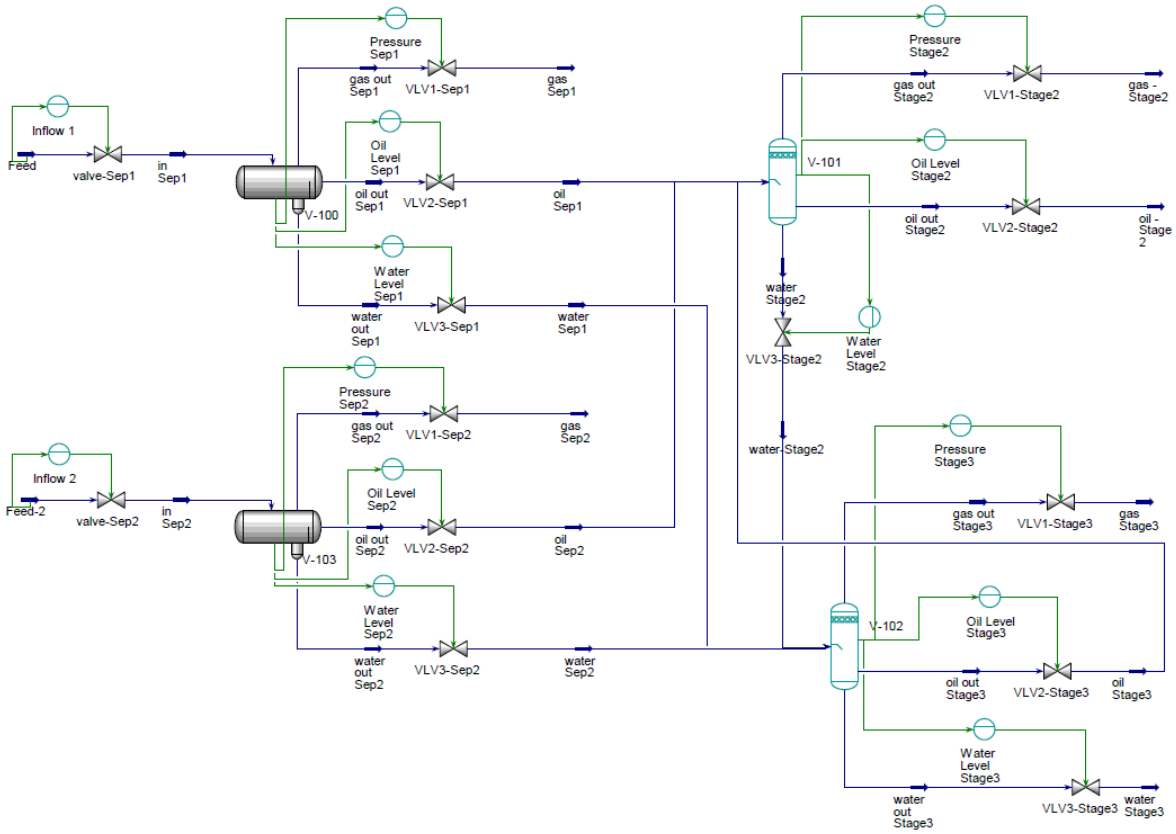

Figure 2. Overall flowsheet model of a gas and oil separation plant.

3.1. First-Stage Separation

The design of the three-phase separators in the first stage was selected as a horizontal vessel with a weir operating at low pressures. The inlet device was set to a reverse distributor with a liquid–vapor separation efficiency of 85 % at the inlet. The same geometrical characteristics were chosen for the two separators. Table 1 shows the geometrical properties and initial conditions.

The inlet conditions were used for the steady-state initialization of the process. The gravity settling model, discussed in more detail in Section 3.8, predicted an outflow of 36 ppm at Separator 1 and of 150 ppm at Separator 2 of oil in the water phase in the steady-state simulations. This value shows that a large part of the oil was already separated in these conditions.

3.2. Second-Stage Separation

The second-stage separator aimed to separate residual water from the oil stream. Water can be present in the oil stream due to poor separation efficiency and entrainment of water in oil. Another reason for the high water residuals are the dynamic changes in water levels during operation, which can lead to a weir overflow of the water to the oil subsystem. The design of this vessel was a vertical cylinder with outflow nozzles at certain heights of

the phases, which settled in the tank. The positioning of the outlet nozzles had to comply with the liquid height setpoints to avoid draining the wrong phase from a nozzle. This tank had more capacity than the three-phase separators and was mainly intended to take in the oil discharges from several three-phase separators in the first stage. The pressure in this unit was set lower than in the three-phase separator units. The geometrical conditions are presented in Table 2.

Table 1. Properties of separators in first stage.

Property	Value	Unit
Length	12	m
Diameter	3	m
Weir Height	1.7	m
Weir Position	9.0	m
Vapor Pressure Setpoint	300	kPa
Water Level Setpoint	1.6	m
Oil Outlet Setpoint *	1	m
Inlet Mass Flow Separator 1	150,000	kg/h
Inlet Mass Flow Separator 2	250,000	kg/h
Inlet Pressure Sep1 & Sep2	500	kPa
Inlet Temp. Sep1 & Sep2	30	°C

* Setpoint in oil subsystem after weir overflow

Table 2. Properties of separator in second stage.

Property	Value	Unit
Height	10	m
Diameter	10	m
Vapor Pressure Setpoint	220	kPa
Water Level Setpoint	2	m
Oil Outlet Setpoint	5	m
Oil Nozzle Location (vertical)	4.7	m
Water Nozzle Location (vertical)	0	m

In the cases of dynamic processes that did not occur frequently and optimally calibrated control units in the preceding stages, weir overflow at stage one rarely occurred, lowering the residence time in these units.

3.3. Third-Stage Separation

The last separation step consisted of a large storage tank with low pressure. In this step, the outcoming oil stream was recycled to the second stage for re-separation. The tank showed no vapor left in the liquid phase in steady-state simulations; therefore, the vapor outlet was used to mimic tank blanketing in the flowsheet model. The geometric properties can be seen in Table 3.

Table 3. Properties of separator in third stage.

Property	Value	Unit
Height	10	m
Diameter	15	m
Vapor Pressure Setpoint	160	kPa
Water Level Setpoint	3	m
Oil Outlet Setpoint	5.5	m
Oil Nozzle Location (vertical)	5	m
Water Nozzle Location (vertical)	0	m

3.4. Compounds

The involved compounds in the process were chosen to represent the properties of natural gas and oil. The components and mole fractions used to model the vapor phase in the process can be seen in Table 4.

Table 4. Composition of Vapor in the Process.

Compound	Mole Fraction
CH4	0.95
N2	0.018
CO2	0.0147
H2S	0.001
C2H6	0.0128
C3H8	0.0029
i-C4H10	0.0001
n-C4H10	0.0002
i-C5H12	0.0002
n-C5H12	0.0001

The heavier hydrocarbons in the crude oil mixture were modeled according to the bulk properties of the oil. Hypothetical compounds were used to model the components of the crude oil. The molecular weight was set to 291.2, and the standard density was chosen to be 900.3 kg/m^3.

3.5. Dynamic Modeling

Different dynamic effects, which were to be considered in the model, occurred during changes of the input parameters of the separation units. These dynamic changes affected the phase volumes entrained in the unit operations and therefore led to different outputs of the units during the time. Aspen HYSYS modeled these changes inside the units, using a virtual stream representing the unit's intrinsic variables. The change in this stream during dynamic operation can be written as:

$$VesselStream = Inflow + VesselStream(PreviousTimeStep) - Outflow \quad (1)$$

At each timestep, a flash calculation was performed on the involved internal vessel stream, which determined the current phases in the unit, and their changes during dynamic simulations. Operational parameters could then be calculated from the results of the flash calculation on the current vessel stream inside the equipment. The flash calculation to define the phase compositions in the involved streams is discussed in the following section.

3.6. Thermodynamic Model

A suitable thermodynamic model is needed to calculate the compositions in the different phases under the current operational parameters. In this work, the Aspen HYSYS inbuilt Peng–Robinson [20] equation was used to calculate the parameters of the involved streams:

$$P = \frac{RT}{V_m - b} - \frac{a\alpha}{V_m^2 + 2bV_m - b^2} \quad (2)$$

where V_m is the molar volume, and the a, b, and α model parameters, which can be expressed by the critical properties and acentric factors of the involved compounds. The compressibility factor Z can be written in a cubic form:

$$Z^3 + (1 - B) \cdot Z^2 + (A - 2B - 3B^2) \cdot Z - (AB - B^2 - B^3) = 0. \quad (3)$$

A and B are defined by the Van der Waals mixing rule, and describe the interactions between the involved molecules. The Rachford–Rice equation can be used to calculate the vapor mole fraction β:

$$\sum_{i=1}^{N} \frac{z_i(\kappa_i - \alpha)}{1 + \beta(\kappa_i - \alpha)} = 0, \tag{4}$$

where N is the number of components in the mixture, z_i is the mole fraction of component i, κ_i is the equilibrium constant for component i, α is the fraction of the mixture that is in the liquid phase, and β is the fraction of the mixture that is in the vapor phase. With the values for κ_i, the fraction of the components in the different phases can be calculated. The exact numerical calculation of this phase composition is an elaborate step, which can be found in numerous works [21].

3.6.1. Vessel Pressure

Vessel pressure at each time step can be determined by the current vapor phase holdup in the vessel. The vessel pressure can be calculated by:

$$P_{Vessel} = \frac{m_{Vapor} RTZ}{M_{Vapor} * (V_{Total} - V_{Liquid})} \tag{5}$$

where m_{Vapor} is the total mass of vapor in the vessel, M_{Vapor} is the molar mass of the vapor, R is the gas constant, and T is the current temperature in the vessel. The compressibility Z was calculated from the Peng–Robinson equation of state, according to Equation (3). Equation (1) was utilized to calculate the mass of vapor, denoted as m_{Vapor}, present in the vessel during each timestep.

3.6.2. Liquid Level

The liquid level in the separation device during dynamic simulation depended on the unit's total volume and the vessel's current intrinsic properties. The liquid holdup at a certain timestep was used to calculate the current liquid height. For a horizontal cylinder, the liquid volume in a cylinder can be calculated by

$$V_{liquid} = cos^{-1}(\frac{r-h}{r})r^2 - (r-h)\sqrt[2]{2rh - h^2}L, \tag{6}$$

where r and L are the radius and length of the horizontal cylinder and h is the height of the liquid phase. Solving this equation for h does not provide an analytical solution; therefore, numerical methods, such as Newton's method, can be used. However, the following simplification can be used to calculate the liquid level in a tank:

$$h = \frac{V_{liquid}}{V_{total}} d_{Vessel.} \tag{7}$$

The height and pressure inside the separation units are used to determine the current output of the vessel. This output is dependent on installed control valves and their desired setpoints at the individual outlets. The application of a suitable control method is mandatory for the dynamic simulation of such processes.

3.7. Process Controls

To analyze the dynamic behavior of the system, suitable control units must be applied to the respective components. The focus of this work was on the water output of the units under dynamic conditions. A liquid height controller was used for calculating the oil and water outputs of the units. To investigate the impact of other properties in the separation units, the vessel pressure was kept at a desired setpoint, because it influenced the static

head contribution of pressure at the output nozzles. A control scheme of a three-phase separator in the flowsheet can be seen in Figure 3.

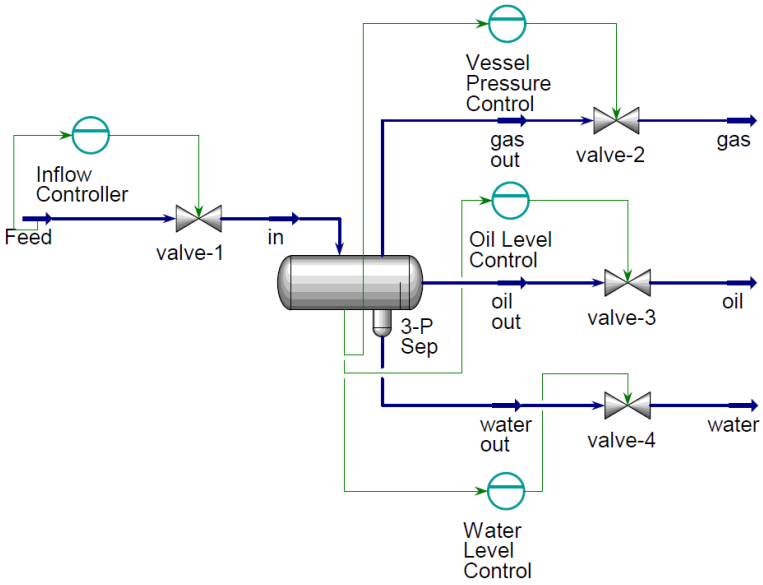

Figure 3. Control scheme of a three-phase separator.

PI controllers were used for controlling the outflow of the units in compliance with the current actuator position of the valve. For controller tuning, the Ziegler–Nichols method was used as a rough estimate. The ultimate gain K_u and ultimate period P_u of the controller were determined using Aspen HYSYS inbuilt methods. The proportional gain K_c and integral period t_{int} were calculated by

$$K_c = \frac{K_u}{2.2} \tag{8}$$

$$t_{int} = \frac{P_u}{1.2}. \tag{9}$$

The characteristics of the valves to respond to input signals from the controllers were set to perform a delayed opening of the valve. The opening rate of the valves was assumed to be linear, with an opening rate of 1% per second. To size the valves for a dynamic process simulation, the nominal flows through the valves that were measured in steady-state operation of the plant were used, and the valve opening was set at 50%. However, if the process parameters changed during simulation, then the opening of the valve changed in order to maintain the desired flow through the valve.

3.8. Gravity Settling

In a multiphase liquid flow, the existing phases in the mixture are usually present as dispersions in the continuous dominating phase. The droplet size distribution of the dispersions can vary depending on the mechanics and parameters in upstream operations. According to the GPSA correlation, the droplet distribution of dispersions, which undergoes mechanical friction in upstream operations, is likely to be between 1–1000 microns. This dispersion of droplets needs to be considered during the sizing of the separation equipment. For the sizing of such equipment, different empirical formulations account for the inflow parameters, as well as the eventual existing separation enhancement units inside the separator. Dispersed droplets will settle in a continuous phase if the buoyant force initiated by the terminal settling velocity is bigger than the drag force on the particle

in the continuous phase. If the terminal velocity is reached, the mass of the particle is in balance with the drag force.

$$F_g = F_{Drag} + F_{Buoyancy}. \tag{10}$$

For a spherical particle with $V = \frac{4}{3}\pi r^3$ as the volume of the particle, the terminal settling velocity can be expressed by

$$v_t = \sqrt{\frac{4 \cdot g \cdot D_{sphere} \cdot (\rho_{sphere} - \rho_{cont})}{3 \cdot \rho_{cont} \cdot C}}. \tag{11}$$

where ρ_{sphere} and ρ_{cont} are the densities of the particle and the continuous phase, and C is the drag coefficient, which depends on the Reynolds number. This drag coefficient is determined mainly by empirical calculations or databases for the different flow regime regions and their Reynolds numbers. Stokes Law can be applied to calculate the terminal velocity for low Reynolds numbers in laminar flow regions:

$$v_{vertical} = \frac{2}{9}\frac{r^2 g(\rho_{oil} - \rho_{water})}{\mu}. \tag{12}$$

The terminal settling velocity can then be used to optimize and size the design of a separation unit. Several sizing methods for various separator designs based on the desired operational values of the equipment are based on the theory of gravity settling [22]: in this approach, a minimum stable droplet diameter is used to calculate the terminal settling velocity of the dispersed droplet from a continuous phase. The separator is then sized accordingly, so that the residence time of the phases inside is larger than the settling time of the dispersion until it rejoins the desired bulk phase level height. Based on the current volume of a phase in the separation unit and the current outflow, the residence time of a phase in the equipment can be estimated by

$$\tau = \frac{V_{Phase}}{V_{Output}}. \tag{13}$$

Under varying parameters of certain process-relevant variables, phase volumes and outflow parameters change during operation, lowering the residence time; therefore, settling efficiencies can drastically change. Sayda et al. [7] used the terminal settling velocity and the calculated residence time under dynamic conditions to evaluate the separation efficiency of the liquid–liquid gravity settling area: smaller particles in the distribution showed a lower terminal settling velocity, which led to a higher discharge of oil in the water phase. With the already-known geometry of the separator, it is possible to determine if a droplet in the water phase will reach the set point (weir height) for separation after a specified distance. Based on the dynamic schedule, this calculation gives information on the oil content at the separator's water outlet. Computational Fluid Dynamics studies on three-phase separators show that the consideration of a Schoepentoeter inlet device shows a high initialization of coalescence in dispersed droplets, which leads to a higher terminal settling velocity [23]. The droplet distribution in the laminar regions remains stable, showing good agreement with the previously mentioned methods.

The terminal settling velocity model, in compliance with predefined geometries for the separation equipment, was used in this study to determine the influence of dynamic operational conditions on the overall water output quality of a gas and oil separation plant.

3.9. Critical Droplet Diameter for Separation

Due to the large volume of the tanks in the second and third stages, long residence can be detected in these units. Using the gravity settling model and the terminal settling velocity, a complete separation of oil and water can be achieved in this separation tank.

Nevertheless, in industrial applications, a small amount of oil in water can still be found. In order to determine trends in the separation efficiency, a minimum stable droplet diameter of 127 microns is assumed [24]. It is assumed that particles smaller than this diameter form a stable emulsion of the oil in water and are not considered separated in this last step.

3.10. Initialization of Droplet Distribution

In order to determine the terminal settling velocities of the dispersed phases, initial assumptions had to be made about the flow properties at the inlets of the separation units. Because of the high water cut in the process when entering the first separation stage, it was assumed that almost the entirety of the oil and gas phases were dissolved in the continuous water phase. Only 1 % of the water existed as a dispersion in the oil phase. Aspen HYSYS allowed these values to be specified when entering the input conditions for the gravity settling model. A Rosin–Rammler distribution was used to model the initial dispersion in the phases. Ref. [25] studied the droplet distribution of gelled crude oil in a hydraulic suspension transport system and showed that the Rosin–Rammler distribution fitted the experimental data under such conditions.

4. Simulation Results

4.1. Dynamic Simulation Scheme

To investigate the reactions of the system to dynamic changes in the input, two different scenarios were chosen. Both scenarios represented a specific situation that can occur during the dynamic operation of a gas and oil separation plant. The first scenario represented a massive increase in the inflow rate in one three-phase separator unit in the first-stage separation process. The second scenario was chosen to be a complete dry startup of Separator 2 (V-103) after maintenance schedules. During both of these scenarios, the oil residuals in the water output of the different stages were monitored. The exact properties and schedules of the dynamic schemes can be seen in Table 5.

Table 5. Parameters for dynamic simulation scheme.

Dynamic Scheme	Monitored Time Frame	Modified Value	Dynamic Event
Case 1	0–120 min	InletFlow 3P-Separator 1 (V-100)	250,000 kg/h at 30 min–150,000 kg/h at 60 min Linear Ramp Duration: 2 min
Case 2	0–90 min	InletFlow 3P-Separator 2 (V-103)	250,000 kg/h at 0 min Linear Ramp Duration: 2 min

Case 1 was monitored during a time frame of 120 min to determine the certain parameter changes inside the units. Case 2 was monitored for 90 min, as stable operation was reached at this time mark. The liquid height in the vessel, and the pressure and outflow rates of the different phases, were monitored.

4.2. Case 1

The incoming mass flow of Separator 1 in the first-stage separation unit was increased from 150,000 kg/h to 250,000 kg/h at the time mark of 30 min. The controller settings for the initiation of this increase were adjusted, so that the increase appeared linearly over a time period of 2 min. At the time mark of 60 min, the inflow rate was changed back to 150,000 kg/h. The incoming feed flow rate of Separator 1 can be seen in Figure 4.

During the dynamic changes, the parameters of the outflow rates of the separation equipment in the first stage were altered. As most of the incoming feed consisted of water, a significant change appeared at the water outlet. As the controllers were tuned to handle such dynamic parameters, only a small overshoot occurred at the water outputs during increase and decrease events. During the adjustment process of the valves at the outputs, a time delay in the process reaction could be seen. The biggest dynamic changes could be

seen in the oil outflow rate because, during the dynamic changes, water overflow in the oil subsection occurred. The changes in the water level can be seen in Figure 5.

The magnitude of the dynamic effects during these changes affects the total mass of water in the oil outlet. A good implementation of the water level control in the first process steps can thus limit the mass of water that has to be separated in the second buffer tank. This influences the design size of the second separation unit and can reduce the total equipment required in the process. Water overflow over the weir with two different tuning methods for the level controller can be seen in Figure 6.

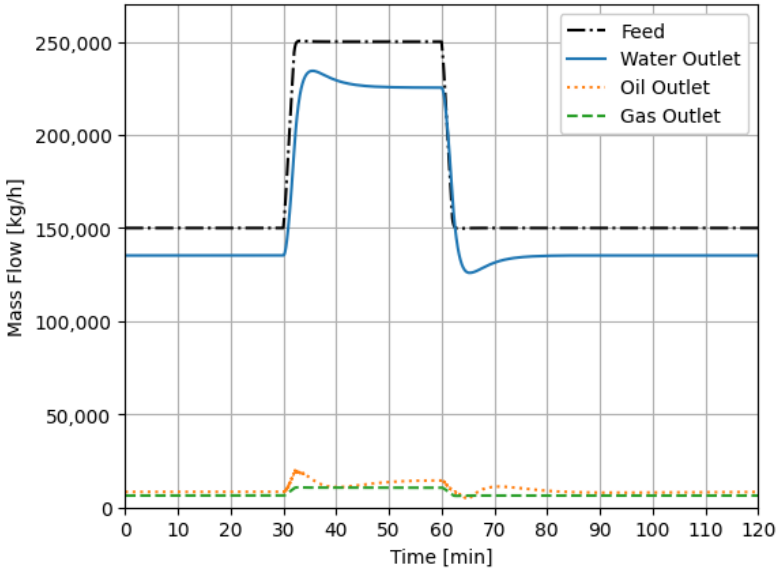

Figure 4. Mass flow rates at Separator 1 in the first stage.

The vessel pressure in Separator 1 during the dynamic changes can be seen in Figure 7. The dynamic changes in the pressure were intercepted relatively quickly by the controller. Pressure changes also affected the mass flow to the water and oil outlets due to the static pressure in the separator.

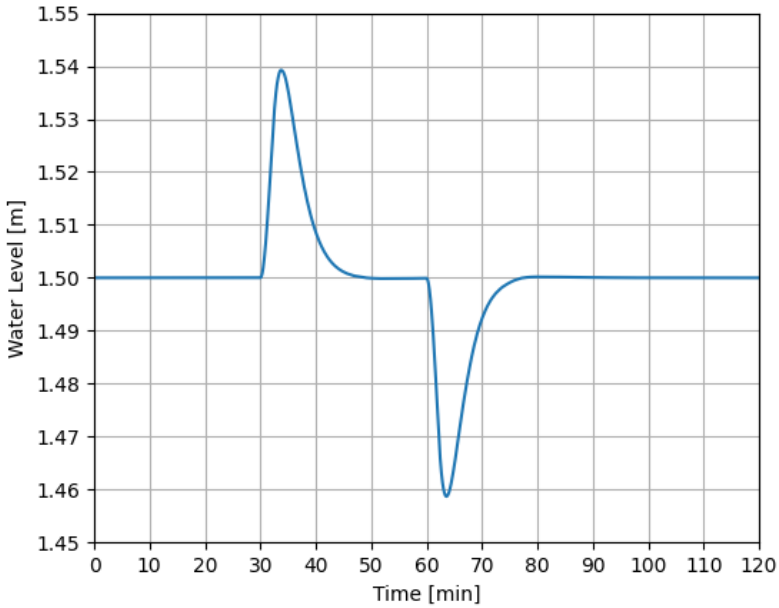

Figure 5. Water level in Separator 1 in the first separation stage.

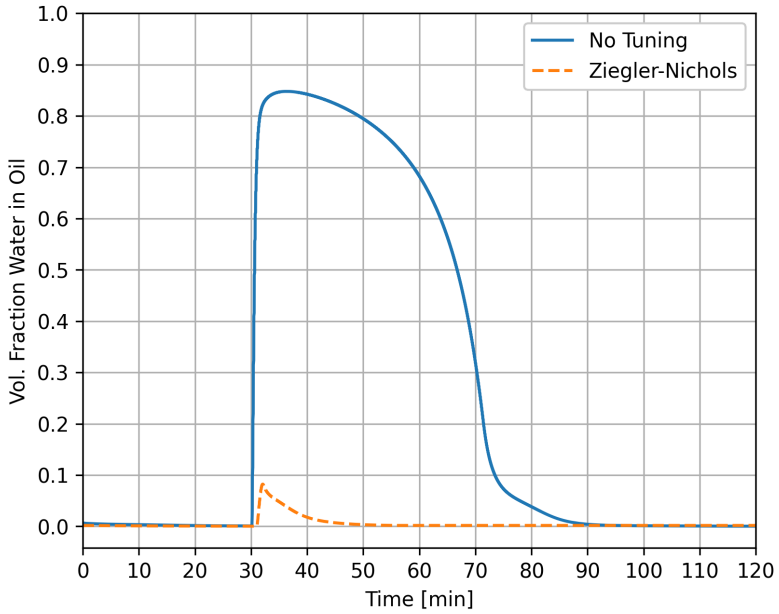

Figure 6. Weir overflow effects under different controllers.

The oil residuals were monitored in three different positions. The water outlet at Separator 1 in the first stage showed a significant increase in oil residuals due to the dynamic change at the input. Separator 2 in the first stage maintained a stable operating point. The second separation stage showed higher oil residuals, due to more incoming fluid from Separator 1 in the first stage. The oil residuals after the first and second separation stages can be seen in Figure 8.

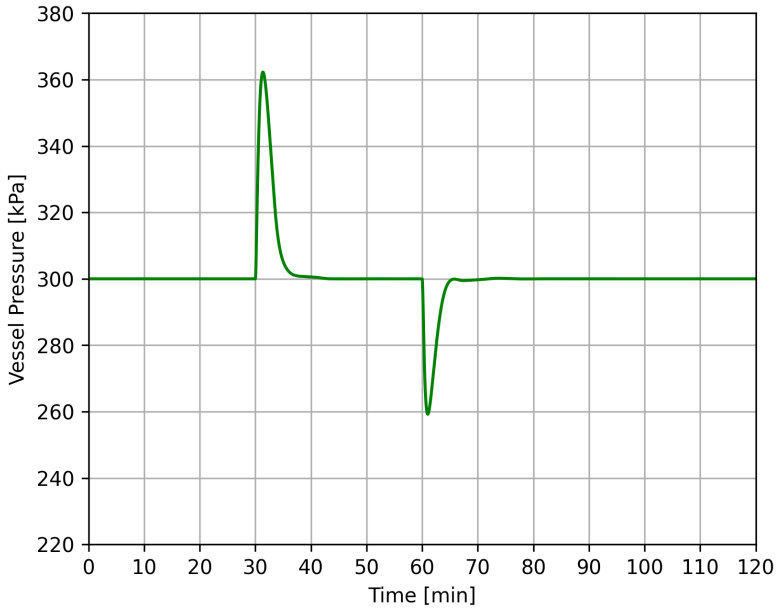

Figure 7. Vessel pressure in Separator 1 in the first separation stage.

During the increase of the inflow rate in Separator 1, the residence time in the third-stage separator was lowered to 1.54 h. In order to achieve a trend curve for separation efficiency, the procedure discussed in Section 3.3 was used. The dynamic changes in the oil residuals in the water output after the third stage of separation can be seen in Figure 9.

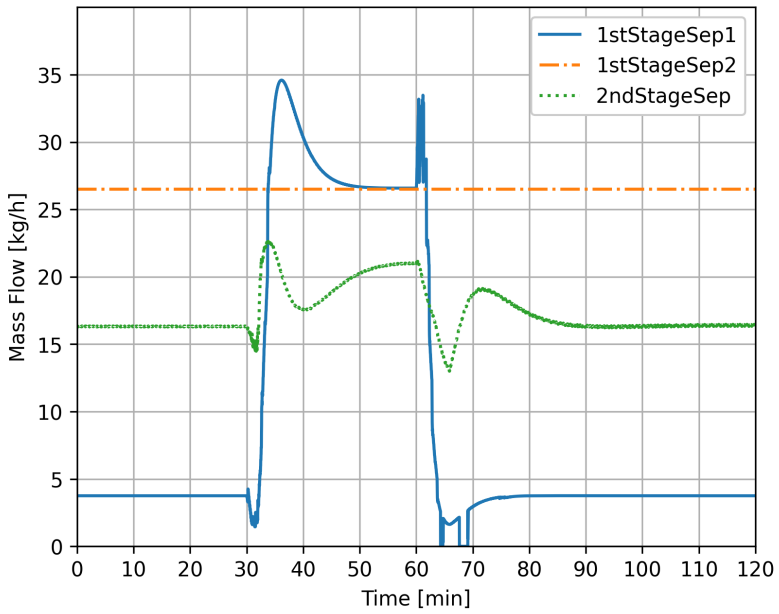

Figure 8. Oil residuals in water output after first and second separation stages.

The change of input shows a large effect on the separation efficiency in the first stage of separation. Due to the control scheme, the weir overflow of water in the oil subsystem of the three-phase separator was not detected in a reasonable enough range to have a noticeable impact on the separation efficiency in the subsequent stages.

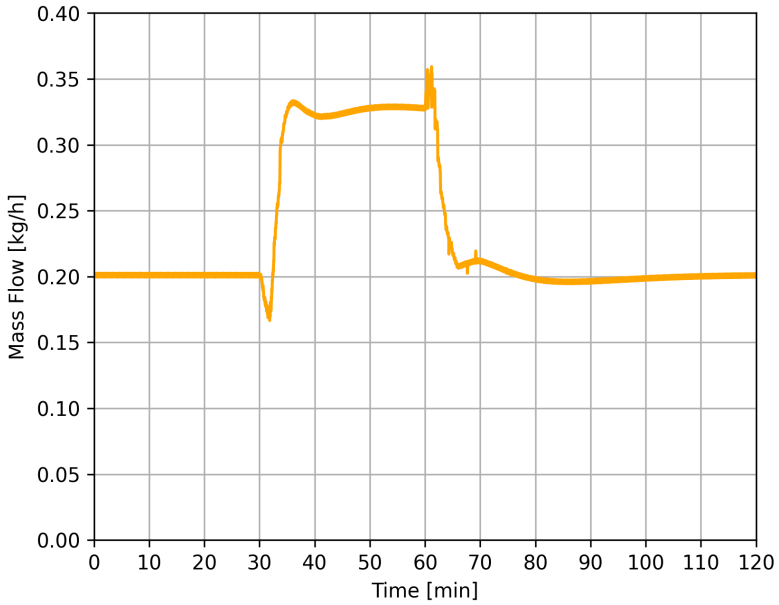

Figure 9. Oil residuals in water output after third separation stage.

4.3. Case 2

A dry start-up of Separator 2 in the first stage was considered in this dynamic scenario. The feed flow rate in Separator 2 was linearly increased from 0 to 250,000 kg/h over a time frame of 2 min. The same parameters as in case 1 were monitored. Water discharge from the vessel started at 8.4 min when the respective setpoint height was reached: at this point, the oil settled on top of the water flows over the weir and filled up the second chamber in the equipment. The setpoint for inducing oil discharge from the vessel was reached at the

time mark of 31.2 min. The mass flow rates at the output of Separator 2 during the start-up can be seen in Figure 10.

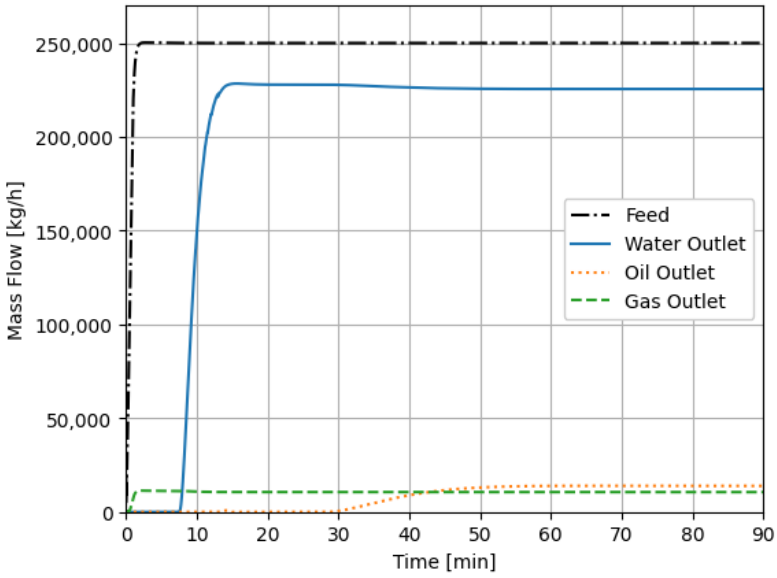

Figure 10. Mass flow rate at Separator 2 in the first stage.

The water level continuously rose until it reached the setpoint of 1.5 meters. Due to the controller tuning, no weir overflow was detectable, which led to no peak water carry-over to the second separation stage. The water level, during the startup of Separator 2, can be seen in Figure 11. During the startup event, the vessel pressure reached maximum, which was then decreased by the controller response and valve opening procedure. The vessel pressure can be seen in Figure 12.

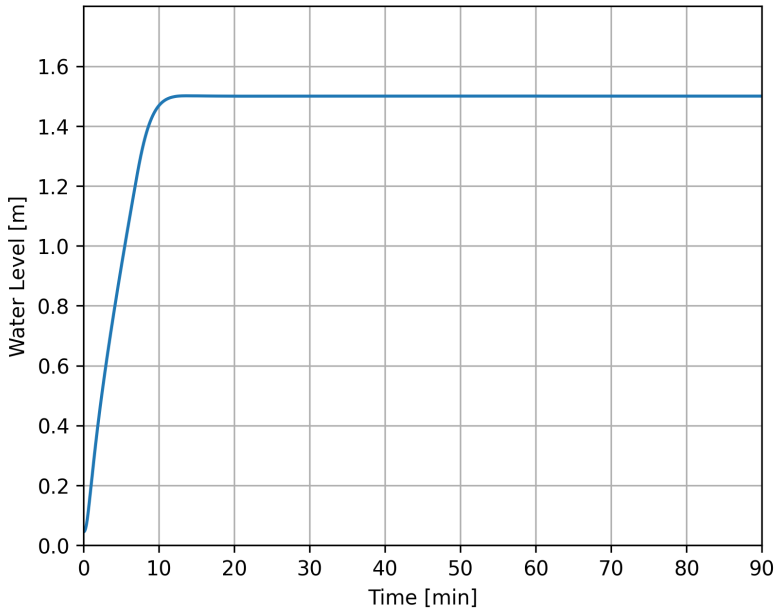

Figure 11. Water level in Separator 2 in the first stage during dry startup.

The oil residuals in the water phase increased in compliance with the water output rate of the unit. A steady-state oil-in-water carry-over in Separator 2 was reached at 25 min, with a calculated oil mass flow in the water phase of 26.9 kg/h. The outflow volume at subsequent stages of separation was initially determined only by the continuously operating Separator 1. After Separator 2 started to discharge water to the storage tank, the

discharge rate of the storage tank increased until it reached a continuous value. The oil residues in the water at the outlet in the third stage were determined using the minimum stable droplet diameter, as in case 1. The oil residuals in the water output of the first- and second-stage separations can be seen in Figure 13.

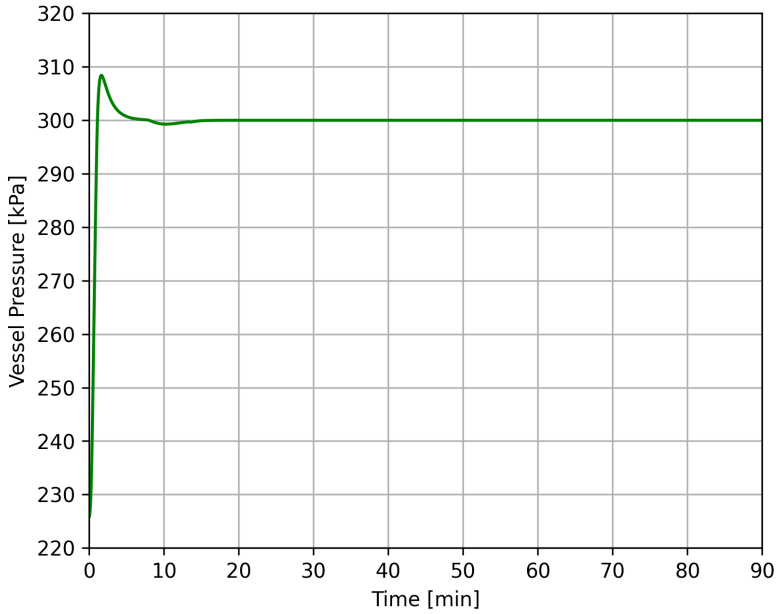

Figure 12. Vessel pressure in Separator 2 at first-stage separation.

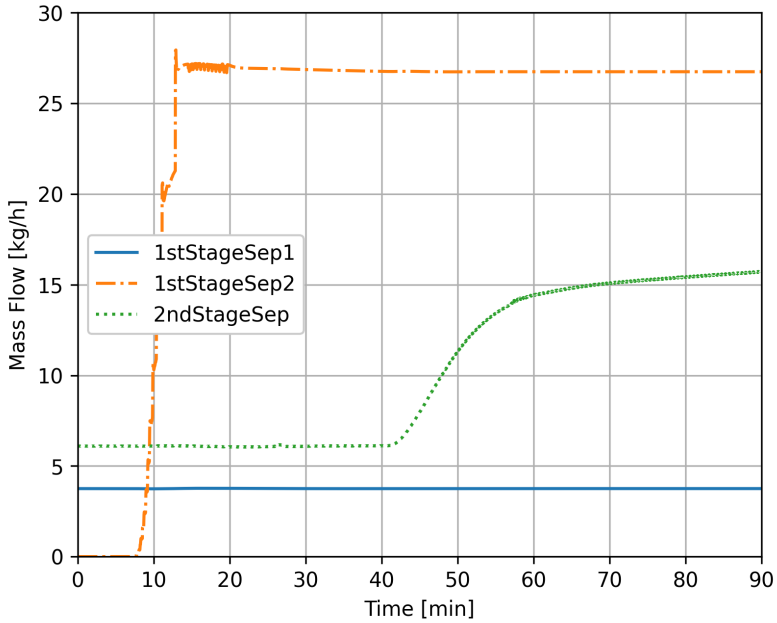

Figure 13. Oil residuals in water output after first- and second-stage separations.

The water output in the last stage maintained a steady level in the first minutes of the simulation, as it was only fed by Separator 1 in the first-stage and second-stage separations. After water discharge at Separator 2 was induced, the outlet flow after the third stage increased until it reached a stable output (Figure 14). The oil residuals, calculated by the minimum stable droplet method (Section 3.3), also increased during the third stage. The oil residuals in the water output in the last stage can be seen in Figure 15.

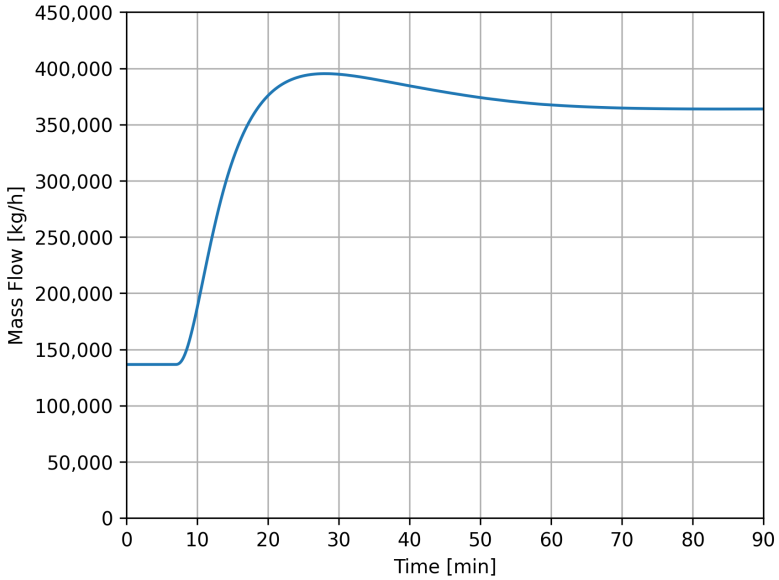

Figure 14. Total water output after third stage.

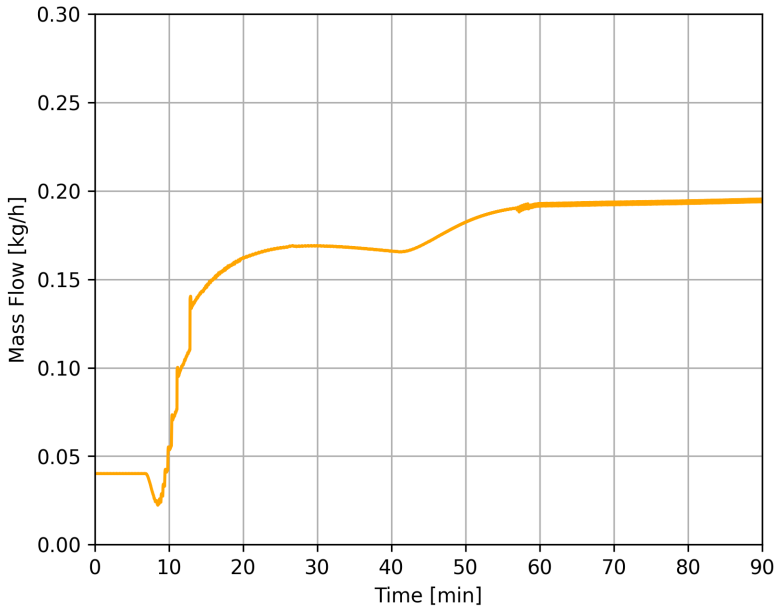

Figure 15. Oil residuals in water output after third-stage separation.

5. Conclusions

A dynamic model of an exemplary gas and oil separation plant was created in Aspen HYSYS. The parameters of the system were measured under different dynamic conditions. A gravity settling model was used to determine the oil residuals in the water output in the first stage of separation. The oil residuals in subsequent stages were modeled by introducing a threshold for the droplet size of separation. The introduction of this threshold enabled a distinction between separated and non-separated droplet sizes and facilitated the analysis of separation efficiencies in the units under dynamic conditions.

Due to the design of the plant components in this example unit, only the three-phase separators showed a significant oil content in the water outlet. The second separation stage, intended as a buffer tank for possible water inclusions in the oil product from the first separation stage, maintained a relatively stable output, as the control units in the previous stages acted quickly enough to prevent peaks in the water-in-oil discharge rate.

This highlights the importance of suitable control systems and reactive units in gas and oil separation plants to reduce equipment costs and enhance production efficiency.

The separation efficiencies and evaluation methods in this modeling approach can be adapted easily to represent values from a real-life plant, and to give feedback on the reaction of the system under dynamic conditions. By integrating this approach with robust validation strategies, predictions of the plant's dynamic behavior can be obtained, which can be used to identify potential optimization strategies for further process intensification.

Author Contributions: Conceptualization, T.J., B.H. and C.J.; data curation, T.J.; formal analysis, T.J.; funding acquisition, M.H.; investigation, T.J.; methodology, T.J. and B.H.; project administration, M.H.; software, T.J.; supervision, B.H., C.J. and M.H.; validation, T.J.; visualization, T.J.; writing—original draft, T.J.; writing—review and editing, B.H. and C.J. All authors have read and agreed to the published version of the manuscript.

Funding: This project received funding from the European Union's Horizon 2020 research and innovation programme under grant agreement No. 871529.

Conflicts of Interest: The authors declare no conflict of interest.

References

1. Olsen, E.R.; Hooghoudt, J.-O.; Maschietti, M.; Andreasen, A. Optimization of an oil and gas separation plant for different reservoir fluids using an evolutionary algorithm. *Energy Fuels* **2021**, *35*, 5392–5406. [CrossRef]
2. Mahmoud, M.; Tariq, Z.; Kamal, M.S.; Al-Naser, M. Intelligent prediction of optimum separation parameters in the multistage crude oil production facilities. *J. Pet. Explor. Prod. Technol.* **2019**, *9*, 2979–2995. [CrossRef]
3. Schei, T.S.; Singstad, P.; Thunem, A.J. Transient Simulations of Gas-Oil-Water Separation Plants. *Model. Identif. Control.* **1991**, *12*, 27–46. [CrossRef]
4. Brambilla, A.; Vaccari, M.; Pannocchia, G. Analytical RTO for a critical distillation process based on offline rigorous simulation. *IFAC-PapersOnLine* **2022**, *55*, 143–148. [CrossRef]
5. Ahmed, T.; Makwashi, N.; Hameed, M. A review of gravity three-phase separators. *J. Emerg. Trends Eng. Appl. Sci.* **2017**, *8*, 143–153.
6. Dionne, M.M. The Dynamic Simulation of a Three Phase Separator. Master's Thesis, University of Calgary, Calgary, AB, Canada, 1998.
7. Sayda, A.F.; Taylor, J.H. Modeling and control of three-phase gravilty separators in oil production facilities. In Proceedings of the IEEE 2007 American Control Conference, New York, NY, USA, 9–13 July 2007; pp. 4847–4853.
8. Grimes, B.A. Population balance model for batch gravity separation of crude oil and water emulsions. part i: Model formulation. *J. Dispers. Sci. Technol.* **2012**, *33*, 578–590. [CrossRef]
9. Backi, C.; Skogestad, S. A simple dynamic gravity separator model for separation efficiency evaluation incorporating level and pressure control. In Proceedings of the American Control Conference, Seattle, WA, USA, 24–26 May 2017; Volume 5.
10. Song, S.; Liu, X.; Li, C.; Li, Z.; Zhang, S.; Wu, W.; Shi, B.; Kang, Q.; Wu, H.; Gong, J. Dynamic simulator for three-phase gravity separators in oil production facilities. *ACS Omega* **2023**, *8*, 6078–6089. [CrossRef] [PubMed]
11. Abdulkadir, M.; Hernandez-Perez, V. The effect of mixture velocity and droplet diameter on oil-water separator using computational fluid dynamics (cfd). In Proceedings of the 7th International Conference on Heat Transfer, Fluid Mechanics and Thermodynamics, Antalya, Turkey, 19–21 July 2010; Volume 61, pp. 35–43.
12. Hallanger, A.; Soenstaboe, F.; Knutsen, T. A Simulation Model for Three-Phase Gravity Separators. In Proceedings of the SPE Annual Technical Conference and Exhibition, Denver, CO, USA, 6–9 October 1996; Society of Petroleum Engineers: Richardson, TX, USA, 1996; Volume 10. [CrossRef]
13. Laleh, A.P.; Svrcek, W.Y.; Monnery, W.D. Computational Fluid Dynamics-Based Study of an Oilfield Separator—Part II: An Optimum Design. *Oil Gas Facil.* **2013**, *2*, 52–59. [CrossRef]
14. Ghaffarkhah, A.; Shahrabi, M.A.; Moraveji, M.K.; Eslami, H. Application of cfd for designing conventional three phase oilfield separator. *Egypt. J. Pet.* **2017**, *26*, 413–420. [CrossRef]
15. Farajzadeh, R.; Zaal, C.; Van den Hoek, P.; Bruining, J. Life-cycle assessment of water injection into hydrocarbon reservoirs using exergy concept. *J. Clean. Prod.* **2019**, *235*, 812–821. [CrossRef]
16. Azizov, I.; Dudek, M.; Øye, G. Emulsions in porous media from the perspective of produced water re-injection—A review. *J. Pet. Sci. Eng.* **2021**, *206*, 109057. [CrossRef]
17. Aspen HYSYS: Process Simulation Software. Available online: https://www.aspentech.com/en/products/engineering/aspen-hysys (accessed on 7 February 2023).
18. Andrade, G.M.; de Menezes, D.Q.; Soares, R.M.; Lemos, T.S.; Teixeira, A.F.; Ribeiro, L.D.; Vieira, B.F.; Pinto, J.C. Virtual flow metering of production flow rates of individual wells in oil and gas platforms through data reconciliation. *J. Pet. Sci. Eng.* **2022**, *208*, 109772. [CrossRef]

19. Vaccari, M.; Pannocchia, G.; Tognotti, L.; Paci, M. Rigorous simulation of geothermal power plants to evaluate environmental performance of alternative configurations. *Renew. Energy* **2023**, *207*, 471–483. [CrossRef]
20. Peng, D.-Y.; Robinson, D. New two-constant equation of state. *Ind. Eng. Chem. Fundam.* **1976**, *15*, 59–64. [CrossRef]
21. Carrero, J. Beyond henry's law in the gas—liquid equilibrium. *ChemTexts* **2021**, *8*, 1. [CrossRef]
22. Arnold, K.; Stewart, M. Chapter 5—Three-phase oil and water separation. In *Surface Production Operations*, 3rd ed.; Arnold, K., Stewart, M., Eds.; Gulf Professional Publishing: Burlington, MA, USA, 2008; pp. 244–315.
23. Kharoua, N.; Khezzar, L.; Saadawi, H. Cfd modelling of a horizontal three-phase separator: A population balance approach. *Am. J. Fluid Dyn.* **2013**, *3*, 101–118.
24. Monnery, W.; Svrcek, W. Successfully specify three-phase separators. *Chem. Eng. Prog.* **1994**, *90*, 29–40.
25. Liu, X.; Wang, Z.; Liu, L.; Wu, C.; Mao, Q. Experimental study on characteristics of oil particle distribution in water-gelled crude oil two-phase flow system. *Adv. Mech. Eng.* **2014**, *6*, 205860.